A Stereoselective, Base-free, Palladium-catalyzed Heck Coupling Between 3-halo-1,4-Naphthoquinones and vinyl-1*H*-1,2,3-Triazoles

Dora C. S. Costa,[a] Luana da S. M. Forezi,[a] Milena D. Lessa,[a] Maicon Delarmelina,[b] Beatriz V. A. Matuck,[a] Maria Clara R. Freitas,[c] Vitor F. Ferreira,[d] Jackson A. L. de C. Resende,[e] José Walkimar de M. Carneiro,*[a] Fernando de C. da Silva*[a]

[a]Universidade Federal Fluminense, Instituto de Química, Campus do Valonguinho, CEP 24020-150, Niterói-RJ, Brazil.

[b]School of Chemistry, Cardiff University, Main Building, Park Place, Cardiff CF10 3AT, United Kingdom.

[c]Universidade Federal Rural do Rio de Janeiro, Instituto de Química, Departamento de Química Fundamental e Inorgânica, Campus Seropédica, CEP 23890-000, Seropédica-RJ, Brazil.

[d]Universidade Federal Fluminense, Departamento de Tecnologia Farmacêutica, Faculdade de Farmácia, 24241-002, Niterói-RJ, Brazil.

[e]Universidade Federal do Mato Grosso, Campus Universitário do Araguaia, Instituto de Ciências Exatas e da Terra, 78698-000, Pontal do Araguaia, MT, Brazil.

*Corresponding Authors: José Walkimar de M. Carneiro (jose_walkimar@id.uff.br); Fernando de C. da Silva (fcsilva@id.uff.br)

Abstract

A stereoselective, base-free Heck coupling between 1,4-naphthoquinone and 1*H*-1,2,3-triazole derivatives was reported for the first time. This study shows that depending on the 1,4-naphthoquinone, the use of an additional base is unnecessary to produce the naphthoquinone-triazole conjugates. This is also the first example of a Heck coupling of these two cores without using a base as an additive. In this work, sixteen new naphthoquinone-triazole hybrids were stereoselectively synthetized in good to excellent yields. The reaction mechanism was discussed based on DFT CAM-B3LYP calculations. The first step is the coordination of the arene to the palladium catalyst to form a palladacycle intermediate. After reorganization in this intermediate, the double bond in the arene is restored to proceed with the coupling step and formation of the C-C bond in the rate determining step. The Kozuchi-Shaik span model was employed to rationalize substituent effects.

Keywords: Lawsone, PEG-400, Pd(OAc)$_2$, cross-coupling, heterocycles, molecular modeling.

Introduction

Several synthetic and natural low-molecular-weight naphthoquinones are used in a broad range of applications in various scientific and technological fields.[1] In this sense, naphthoquinones have been shown to have diverse bioactivities including, anticancer, [1] anti-oral squamous cell carcinoma,[2] molluscicidal,[3,4] antiparasitic,[5-7] antimalarial,[8] antileishmanial,[9] anti-inflammatory,[10] antifungal,[11] antimicrobial[12] and trypanocidal activities.[13]

On the other hand, heterocycles, such as triazoles, are considered privileged structures in medicinal chemistry because they are incorporated into the cores of many commercially available drugs.[14] From the earliest days of medicinal chemistry, these heterocycles were known to be important pharmacophores in many bioactive compounds.[15] 1,2,3-Triazoles are not natural but have become an important class of compounds that have been investigated for the treatment of several important diseases[16,17] as they have been shown to have antiviral,[18] antifungal,[19] anti-inflammatory,[20] antibacterial[21] and antitumoral activities.[19,22-24]

Whereas the naphthoquinone and 1,2,3-triazole scaffolds are both of major importance individually, molecules containing these two moieties have been studied in recent years against various diseases, *i.e.,* to determine their antitumor activity, showing that this molecular combination potentially offers great synergism. [19,25,26]

Several reaction types involving changes in the lapachol side chain have been described for the preparation of naphthoquinone-triazole hybrids.[1] This kind of derivatives can be obtained through the construction of a carbon-carbon bond at C-3 of a 1,4-naphthoquinone.

Palladium-catalyzed coupling reactions between alkenes and aryl halides, known as Mizoroki-Heck reactions (or simply Heck reactions), are among the most important methods to construct carbon-carbon bonds, and they have been extensively used in the synthesis of natural products in the pharmaceutical industry and in bioorganic chemistry.[27,28] In fact, the Heck coupling reaction has already been applied in the synthesis of lapachol analogues, as reported by Perez and coworkers[29] for the synthesis of *C*-alkenyl derivatives from the Heck coupling of 2-hydroxy-3-iodo-1,4-naphthoquinone with electron-deficient alkenes. However, to the best of our knowledge, there are no reports of

a Heck coupling between a naphthoquinone and a triazole nuclei, which makes the study of such reaction quite attractive.

Herein, we report the first synthesis and methodological study of a stereoselective, base-free, palladium-catalyzed Heck coupling, between naphthoquinones and 1*H*-1,2,3-triazoles. Density Functional Theory (DFT) was additionally employed to carry out an extensive analysis of the reaction mechanism for the alkene-naphthoquinone coupling step.

Results and Discussion

Synthesis and Characterization Studies

Initially, it was necessary to prepare 3-halide-1,4-naphthoquinones **3a-b** and 4-vinyl-1*H*-1,2,3-triazoles **5a-h** (Scheme 1). These compounds were prepared according to methodologies reported in the literature. For that, naphthoquinones **2a** and **2b** were synthesized from 2-hydroxy-1,4-naphthoquinone (**1**) – Scheme 1A – and the obtained derivatives presented spectroscopic data in good agreement with already reported values.[30],[31],[32,33] By its turn, 4-vinyl-1*H*-1,2,3-triazoles (**5a-h**) were prepared[19,34] based on a variant of the Huisgen 1,3-dipolar cycloaddition protocol – Scheme 1B – and all triazolic derivatives presented spectroscopic data consistent with reported values.[19,34]
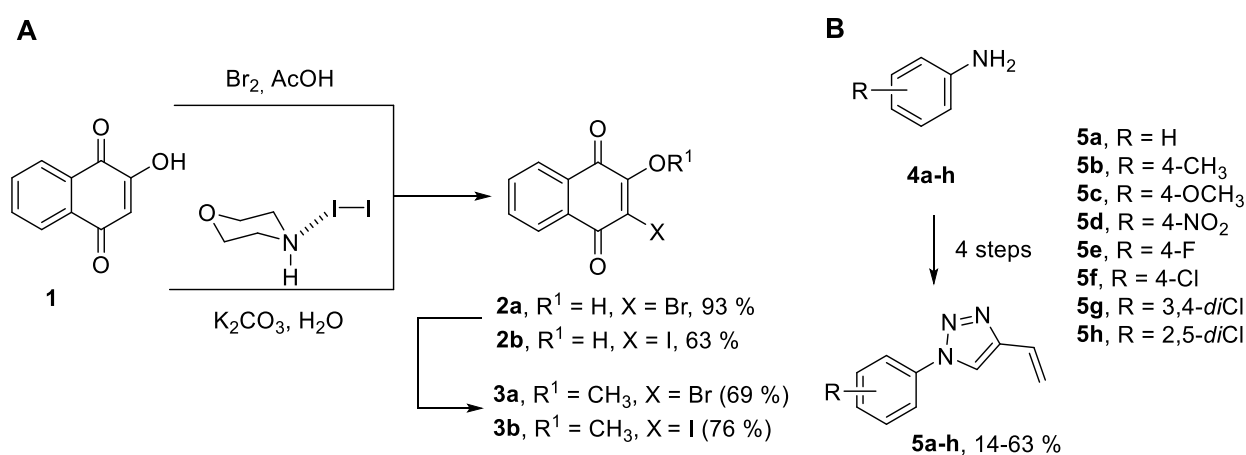

Scheme 1. Synthesis of compounds: **A.3a**, **3b** and **B. 5a-h**

4

Following the previous preparative steps, we started our study using the 4-vinyl-1*H*-1,2,3-triazoles (**5a-h**) to evaluate the influence of the aromatic ring substituents on the course of the Heck coupling reaction. The first attempts to couple 3-halide-2-methoxy-1,4-naphthoquinones (**3a-b**) and **5a** were carried out according to previously described conditions for this type of coupling.[35,36]

For that, 3-bromo-2-methoxy-1,4-naphthoquinone (**3a**) and 4-vinyl-1*H*-1,2,3-triazole **5** (1.1 equiv.) were reacted under the catalysis of palladium (50 mol% Pd(OAc)$_2$) using PPh$_3$ as a ligand (2.0 equiv.) in the presence of K$_2$CO$_3$ in a mixture of toluene/DMF (2:1) at 95 °C (Table 1, entry 1). The reaction was monitored by TLC, and after 60 min., the starting naphthoquinone had been consumed. The formation of **6a** was successfully achieved in 88 % yield and its structure was fully characterized. It should be noted that a crystal of **6a** was grown, and the analysis by X-ray crystallography (see the Supplementary Material) confirmed that the product was exclusively obtained as the *E* stereoisomer (Figure 1).

Table 1. Study of the reaction conditions for the synthesis of Heck products **6a-h**.

3a, X = Br
3b, X = I

6a-h
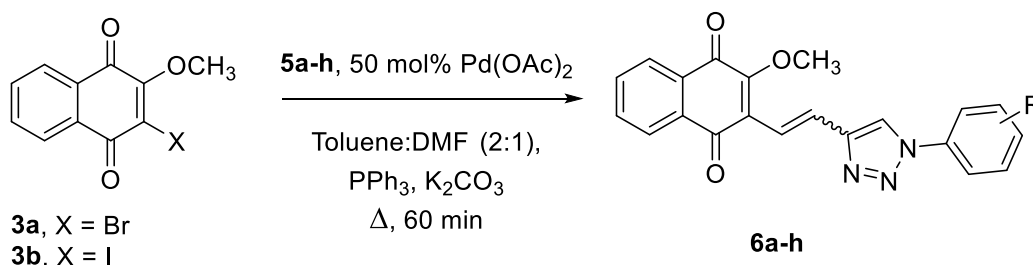
Entry	R	X	Ph$_3$P (equiv.)	T (°C)	Ratio (*E/Z*)	Product (η$_{isolated}$)
1	H	Br	2.0	95	1:0	**6a** (88 %)
2	H	Br	2.0	120	1:0	**6a** (65 %)
3	H	Br	1.5	95	1:0	**6a** (38 %)
4	4-CH$_3$	Br	2.0	95	4:1	**6b** (70 %)
5	4-OCH$_3$	Br	2.0	95	-	**6c**[(a)]
6	4-NO$_2$	Br	2.0	95	2:1	**6d** (28 %)
7	4-F	Br	2.0	95	1:1.5	**6e** (16 %)
8	4-Cl	Br	2.0	95	1:0	**6f** (60 %)
9	3,4-*di*Cl	Br	2.0	95	1:1.5	**6g** (16 %)
10	2,5-*di*Cl	Br	2.0	95	1.5:1	**6h** (39 %)
11	H	I	2.0	95	1:0	**6a** (69 %)[b]
12	4-CH$_3$	I	2.0	95	1:0	**6b** (55 %)[c]

[(a)]No Heck product formation detected; degradation of **5c** was observed; [(b)]**6a** contaminated with PPh$_3$ + other byproducts. [(c)]**6b** contaminated with PPh$_3$ + other byproducts.
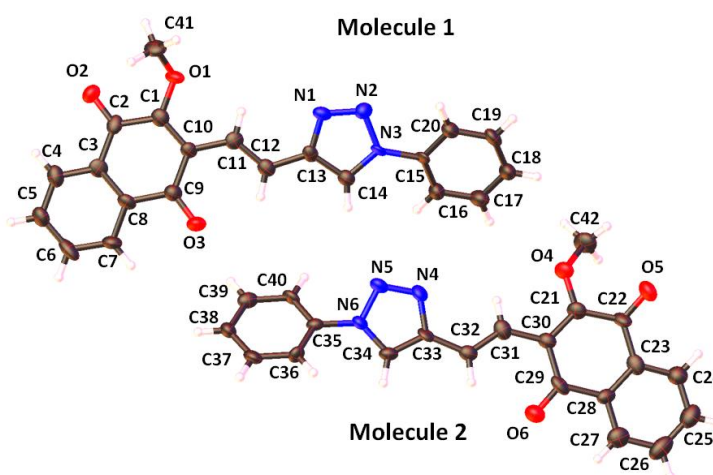
Figure 1. *ORTEP* diagram of **6a**.

Entries 2 and 3 of Table 1 indicate that increasing the temperature (entry 2) and decreasing the amount of PPh$_3$ ligand (entry 3) reduced the yield of the reaction. However, subjecting the remaining 4-vinyl-1*H*-1,2,3-triazoles to the conditions of entry 1 resulted in mixtures of *E*/*Z* stereoisomers in 4:1 (Table 1, entry 4), 2:1 (Table 1, entry 6) and 1.5:1 (Table 1, entry 10) ratios when **5b**, **5d** and **5h**, respectively, were employed. When triazole **5f** was used, similarly to the outcome with **5a**, the reaction resulted in product **5f** as the single stereoisomer *E* in 60 % yield (Table 1, entry 8).

It should also be noted that product **6c** from the reaction with triazole derivative **5c** has not been identified (Table 1, entry 5). Derivatives **6e** and **6g** were obtained in an inverted ratio of 1.0:1.5; that is, the *Z* isomers was the major species (Table 1, entries 7 and 9). After slow crystallization at low temperature (from chloroform/hexane), compounds **6b**, **6d** and **6h** were obtained as *E* stereoisomers only. The configuration was determined by ^{1}H NMR spectroscopy based on the two characteristic doublets at 7.61 (d, *J* 16.6 Hz, 1H) and 8.05 ppm (d, *J* 16.6 Hz, 1H), corresponding to the two vinyl hydrogens (see the Supporting information for details). However, products **6e** and **6h** could not be obtained in the form of a single stereoisomer. All attempts for crystallization resulted in the recovery of stereoisomeric *E*/*Z* mixtures in the initial ratio.

We subsequently studied the effect of the halogen at C-3 by reacting 2-methoxy-3-iodo-1,4-naphthoquinone (**3b**) with **5a** (Table 1, entry 11) and **5b** (Table 1, entry 12). This approach allowed the exclusive synthesis of Heck products (*E*)-**6a** and (*E*)-**6b**; however, the products were contaminated with residual PPh$_3$ and other byproducts.

Considering the production of stereoisomeric mixtures and the low yields, it was decided to investigate the effect of the reaction solvent in combination with the effect of the halogen at the C-3 position of the naphthoquinone.

Recently, polyethylene glycol (PEG) has been widely used in C-C bond formation catalyzed by palladium. PEG-400 is commercially available and has a low environmental impact.[37] In addition, it has also been used in stereoselective reactions catalyzed by palladium in the absence of a ligand.[27,28] It has been proposed that PEG helps reducing Pd^{2+} to Pd^{0}, turning over the catalytic cycle through the oxidation of terminal hydroxyl groups to aldehydes.[37] Thus, we decided to include PEG-400 as a solvent and adjuvant in this reaction.

The employed methodology was adapted from Demidoff and coworkers;[27] we reacted naphthoquinone **3a** and vinyl triazole **5a** with 15 mol% Pd(OAc)$_2$, PEG-400 and NaOH (Table 2, entry 1). The product was identified as (*E*)-**7a**, obtained in 46 % yield. With this result, we decided to remove the base from the reaction medium, once it apparently allowed basic hydrolysis by nucleophilic substitution of the methoxy group at C-2. These different reaction conditions (Table 2, entry 2) afforded the desired product **6a** in 10 % yield with recovery of 27 % of the starting material **3a** after 1 h reaction time (Table 2, entry 2).

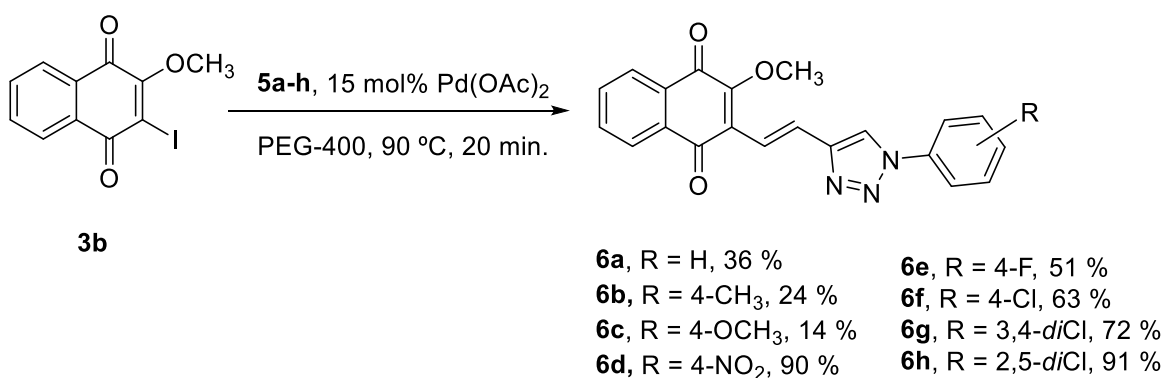**Table 2.** Study of the reaction conditions for the synthesis of Heck products **6a**.
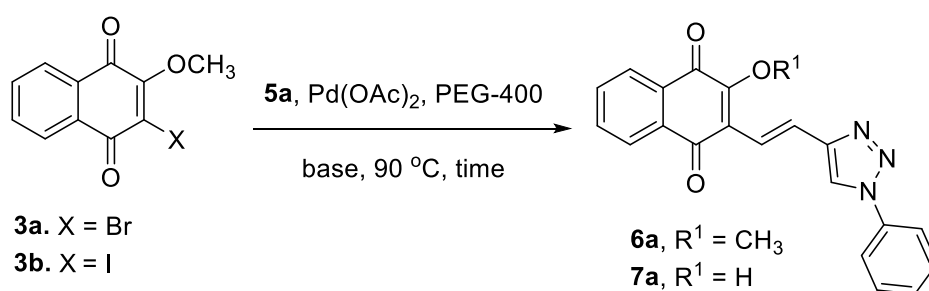
Entry	X	Pd(OAc)$_2$ (mol%)	Base	t (min.)	Product ($\eta_{isolated}$)
1	Br	15	NaOH	30	**7a** (46 %)
2	Br	15	-	60	**6a** (10 %)[a]
3	I	15	-	20	**6a** (36 %)
4	I	10	-	20	**6a** (27 %)[b]

[a]with 27 % of **3a** recovered; [b]with 25 % of **3b** recovered

Thus, we evaluated the behavior of the reaction when iodinated naphthoquinone **3b** was used in the presence of PEG-400. Derivative **3b** was reacted with **5a** in the presence

of 15 mol% Pd(OAc)$_2$ and PEG-400 at 90 °C in the absence of ligand and base (Table 2, entry 3). Product **6a** was obtained as the *E* isomer in 36 % yield. The structure of **6a** was confirmed by HRMS-ESI which showed a peak at m/z 380.100683 (M+Na). It should be noted that decreasing the loading to 10 mol% palladium catalyst does not allow the complete conversion of **3b** into **6a**, resulting in lower yield (Table 2, entry 4).

The conditions (Table 2, entry 3) for obtaining the stereoselective Heck coupling (*E*)-product were applied to **5b-h**, allowing to synthesize (*E*)-**6b-h** as a sole product in 14-91 % yields (Scheme 3). Products containing electron-donating groups on the aromatic ring (**6b** and **6c**) were obtained in much lower yields (24 % and 14 %, respectively) than those containing electron-withdrawing groups (**6e** and **6h**), which were obtained in 51 % and 91 % yields, respectively (Scheme 3).
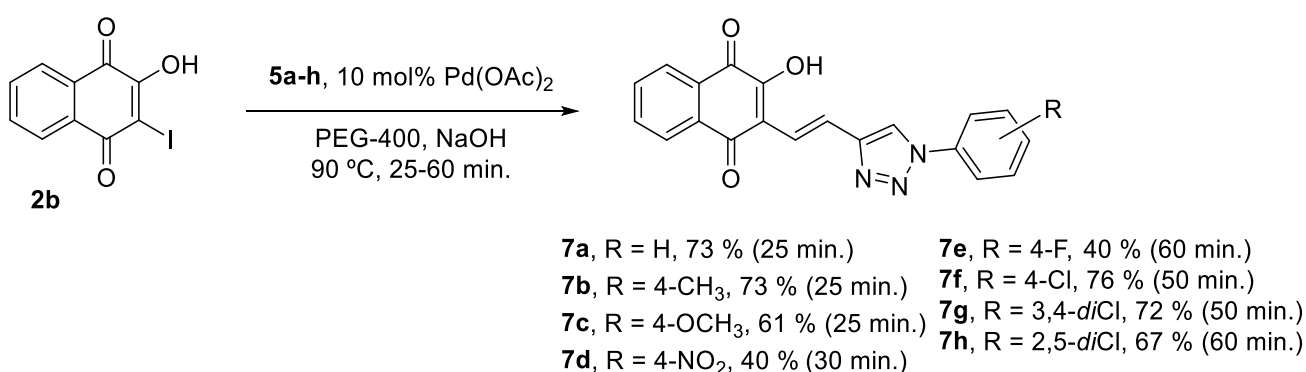

6a, R = H, 36 %   **6e**, R = 4-F, 51 %
6b, R = 4-CH$_3$, 24 %   **6f**, R = 4-Cl, 63 %
6c, R = 4-OCH$_3$, 14 % **6g**, R = 3,4-*di*Cl, 72 %
6d, R = 4-NO$_2$, 90 %   **6h**, R = 2,5-*di*Cl, 91 %

Scheme 3. Stereoselective synthesis of **6a-h** by Heck coupling.

Considering that we obtained derivative **7a** (Table 2, entry 1) when NaOH was used, we decided to open the range of this study to the synthesis of **7a-h** derivatives. So, we moved on with this investigation, reacting 2-hydroxy-3-iodo-1,4-naphthoquinone (**2b**) and 1-phenyl-4-vinyl-1*H*-1,2,3-triazole (**5a,** 1.0 equiv.) using the same base- and ligand-free conditions using PEG-400 and 15 mol% Pd(OAc)$_2$ as catalyst at 90 °C. However, no Heck product **7a** was detected. An attempt to use excess **5a** (4.0 equiv.) afforded traces of Heck coupling product **7a**.

At this point, we decided to return to the conditions described by Demidoff *et al.*,[27] that is, using an inorganic base (NaOH) and performing the reaction between **2b** and **5a** with PEG-400, NaOH (3.0 equiv.) and catalytic Pd(OAc)$_2$ (10 mol%) at 90 °C in the absence of ligand. After 25 min, we obtained **7a** in 73 % yield (Scheme 4).

The ^{1}H NMR spectrum showed two doublets at 7.71 ppm (d, J 16.4 Hz, 1H) and 8.07 ppm (d, J 16.4 Hz, 1H) with the same coupling constant, indicating the exclusive formation of (E)-**7a**. Furthermore, HRMS-ESI(-) showed a peak at m/z 342.087775 for [M-H]$^-$ (calcd for $C_{20}H_{12}N_3O_3$, 342.088415, see the Supporting information for details). Thus, we extended the reaction to **5b-h**, and only (E)-**7b-h** were identified (Scheme 4). The reaction times ranged from 25 to 60 minutes, and the 4-vinyl-1H-1,2,3-triazoles with electron-donating groups on the aromatic ring (**7b** and **7c**) or two chloro substituents (**7g** and **7h**) provided higher yields (61-74 %) when compared to the derivatives with electron-withdrawing groups, as 4-NO$_2$ (**7d**) and 4-F (**7f**) did not exceed 40 % yield (Scheme 4).

7a, R = H, 73 % (25 min.)   **7e**, R = 4-F, 40 % (60 min.)
7b, R = 4-CH$_3$, 73 % (25 min.)   **7f**, R = 4-Cl, 76 % (50 min.)
7c, R = 4-OCH$_3$, 61 % (25 min.) **7g**, R = 3,4-diCl, 72 % (50 min.)
7d, R = 4-NO$_2$, 40 % (30 min.)   **7h**, R = 2,5-diCl, 67 % (60 min.)

**Scheme 4.** Stereoselective synthesis of **7a-h** by Heck coupling.

The experimental results discussed above show that the coupling reaction between the triazole and the naphthoquinone occurs when the classical methodology is used, i.e., PPh$_3$ as a ligand and K$_2$CO$_3$ as a base (Table 1). However, in the absence of either ligand (Scheme 4) or both base and ligand (Table 2 and Scheme 3), using PEG-400 as the solvent, the reaction was also successful. For the reaction using the classical methodology, both electron withdrawing and electron donating groups substituted in the aromatic ring of the triazole reduces the reaction yield (Table 1). For the reaction where both ligand and base are absent, electron withdrawing groups leads to higher reaction yields (entries **6d-h**, Scheme 3), although the reverse was observed for the reaction between **2b** and **5a-h**, using PEG-400 and NaOH in the absence of a ligand (see, for example, entries **7d-e**, Scheme 4). Considering that the presence of a base has been taken as critical to the turnover of the catalytic cycle of the Heck coupling, as it regenerates the supposed active palladium species [Pd^0], we hypothesized that the free electron pairs of the N-2 or N-3 nitrogen atoms of the 4-vinyl-1H-1,2,3-triazoles **5a-h** might function as an organic base in

these reactions. This would also justify why the reaction occurs when using naphthoquinone **3b** and does not occur when using naphthoquinone **2b**. For **2b**, the acidic hydrogen of the hydroxyl group of C-2 would neutralize the basic function of the triazole, preventing it to work as the required base, a condition that is regenerated in the presence of the stronger base NaOH.

Computational Investigation Studies

In the last stage of this investigation, a detailed computational study was carried out to shed light on the possible catalytic mechanism, as well as to try rationalizing the effect of the substituents in the 4-vinyl-1*H*-1,2,3-triazole derivatives on the reaction yield.
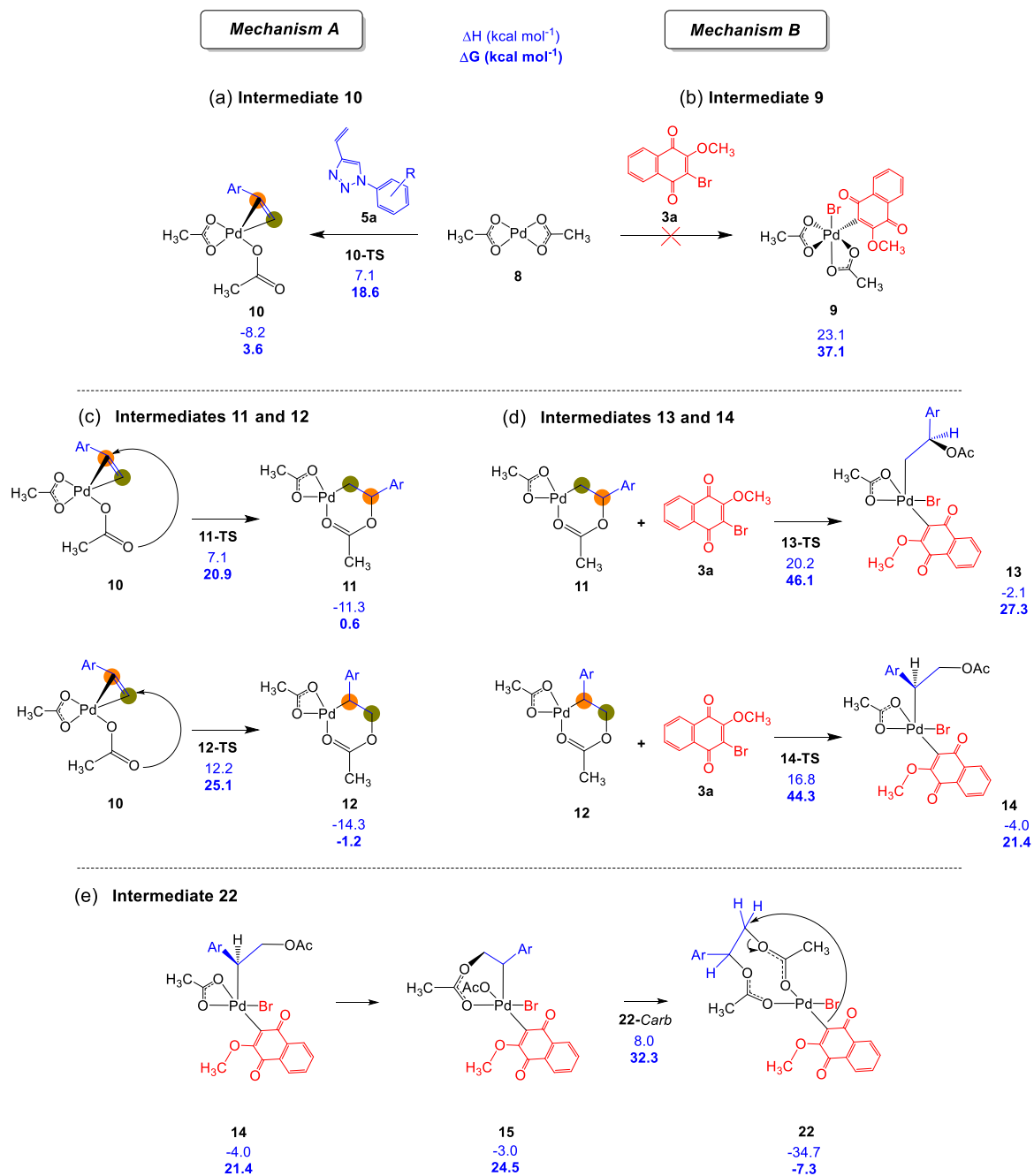
The mechanism for the palladium-catalyzed Heck reaction has been widely investigated recently.[38,39] The most accepted mechanism for this reaction is based on the coupling between an aryl or vinyl halide and an alkene. In the presence of a base and a ligand (usually triphenylphosphine, PPh$_3$), Pd^{2+} may be reduced to Pd^0, leading to the formation of the active palladium catalyst. This reduced Pd^0 can then enter the catalytic cycle by oxidative addition to the C-X bond, forming a palladium complex intermediate, on which the olefin can coordinate to proceed with the C-C bond formation.[27] According to this mechanism, the formation of Pd^0 (or palladium black) in the reaction mixture is expected. As Pd^0 has sometimes not been observed during the reaction course, Yao *et. al*[40] proposed an alternative mechanism, in which the olefin first reacts with the palladium catalyst - Pd(OAc)$_2$ - to form intermediate **11** (Scheme 5), the so-called palladacycle intermediate, which would then react with the aryl halide, leading to the C-C bond-forming step. These two alternatives are represented in Scheme 5.
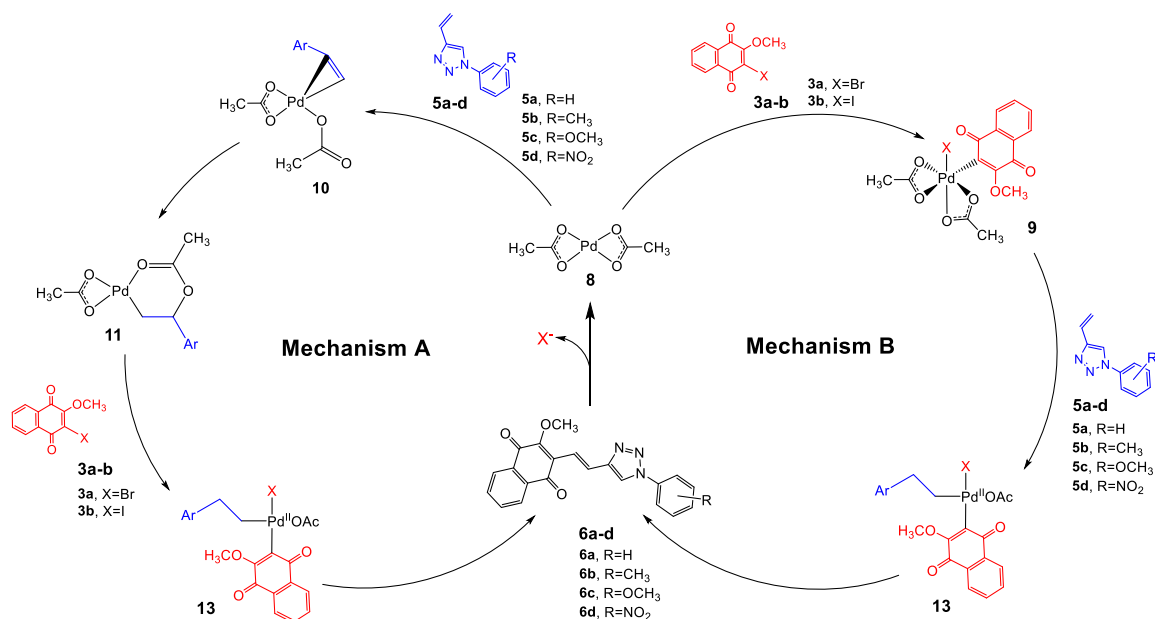
Scheme 5. Putative mechanism for palladium-catalyzed Heck reaction via palladacycle intermediate formation (Mechanism A), as proposed by Yao *et al.*[40], and, classical mechanism for Heck reaction (Mechanism B).

Considering these two hypotheses, both mechanisms were investigated in the present study. We initially considered the first step of mechanism B (Scheme 6b), the oxidative addition of the naphthoquinone **3a** to Pd(OAc)$_2$, leading to the formation of intermediate **9**. According to our calculation, this is an *endothermic* step, with relative enthalpy of 23.1 kcal mol^{-1}. On the other hand, for the first step of mechanism A (Scheme 6a), coordination of the alkene on the Pd(OAc)$_2$ to form intermediate **10**, we computed an *exothermic* process (by -8.2 kcal mol$^-$), with a corresponding activation enthalpy (**10-TS**) of 7.1 kcal mol^{-1}. Therefore, the initial steps for the two alternatives have clear different behavior.

Although highly exothermic processes have been reported for the reaction between Pd^0 and naphthoquinones, a correspondingly high-temperature change was not observed.[41] In addition, significant experimental data did not show the formation of palladium black, or Pd^0, during the reaction course.[40] Considering these facts and the present finding that the direct addition of naphthoquinone to Pd(OAc)$_2$ is unfavorable, we continued our study considering the coordination of the alkene to the palladium catalyst Pd(OAc)$_2$) in the first step of the reaction (Mechanism A, Scheme 5). However, it is important to note that both mechanisms converge to a common intermediate (**13** or **14**, see discussion below), which will finally lead to the formation of the C-C bond.

Scheme 6. (a) First step (1) of **Mechanism A** – Coordination of the alkene to the palladium catalyst for the formation of intermediate **10**. **(b)** First step (1) of **Mechanism B** – Formation of the intermediate **9** in an endothermic process. **(c)** Second step of **Mechanism A** – Formation of palladacycle intermediates **11** and **12**. **(d)** Third step of **Mechanism A** – Insertion of the naphthoquinone into the palladium complex to form intermediates **13** and **14**. **(e)** Formation of the intermediate **22** via **15**.

Following mechanism A, after coordination of the alkene to the Pd(OAc)$_2$ catalyst (**10**, exothermic by 8.2 kcal mol^{-1}, activation enthalpy of 7.1 kcal mol^{-1}), there occurs the formation of the palladacycle intermediate (**11** or **12**), via the nucleophilic attack of the acetate oxygen either on the primary or on the secondary carbon of the coordinated alkene, forming two possible palladacycle-intermediates: **11**, which has the primary carbon of the alkenyl group coordinated to the palladium, with relative enthalpy of -11.3 kcal mol^{-1} and activation enthalpy (**11-TS**) of 7.1 kcal mol^{-1}; **12,** which has the secondary carbon of the alkenyl group coordinated to the metal center, with relative enthalpy of -14.3 kcal mol^{-1} and activation enthalpy (**12-TS**) of 12.2 kcal mol^{-1} (Scheme 6c). The relative enthalpies of the intermediates (**11** *vs* **12**) are close to each other (**12** more stable by about 3.0 kcal mol^{-1}), while the activation enthalpy to form **12** (**11** *vs* **12**) is higher by about 5.0 kcal mol^{-1}.

The next step is the oxidative addition of the naphthoquinone to the palladacycle intermediate formed in the previous step. Starting from **11** and **12**, intermediates **13** and **14** are formed in an exothermic process (by -2.1 and -4.0 kcal mol^{-1}, respectively). For this insertion, we computed activation enthalpies of 20.2 kcal mol^{-1} (**13-TS**) and 16.8 kcal mol^{-1} (**14-TS)** (Scheme 6d), respectively. The bond between the palladium atom and the secondary carbon of the alkene (**14**) is more stable than the corresponding bond with the primary carbon. Up to this point, the results suggest the preferential formation of intermediate **14**.

Intermediates **13** and **14** (Scheme 6d) are key intermediates in this mechanism, whose formation involves activation barriers that are among the highest calculated here. Additionally, intermediates **13** and **14** precedes the most important step in this mechanism, the formation of the C-C bond. Considering the large number of rotatable bonds, with the consequent high conformational flexibility, an extensive number of isomers were considered to identify the most stable one for intermediates **13** and **14** (see also Fig. S94 and Fig. S95 in the Supplementary Material). All attempts to optimize these intermediates with a planar squared geometry were unsuccessful (the optimized geometries of these intermediates with octahedral and square pyramidal arrangements are shown in Fig. S94 of the Supporting information). The squared pyramidal geometry shows the lowest energy, with the triazole in the axial position and the acetate, the naphthoquinone, and the bromide ion in the equatorial positions.

In addition to the exhaustive comparison of conformers, as described above, the possible displacement of the labile ligands due to chemical equilibrium in solution was

further considered. Species **16** (see Figs. S96, S98, and S100 in the Supporting information for a description of structures **16**, **18** and **20**) may be obtained by elimination of AcO⁻, whereas species **18** may be formed by elimination of Br⁻. Finally, species **20** may be formed by elimination of one of the acetate ions, accompanied by alkene deprotonation. Species **16**, **18** and **20** have relative enthalpies of 59.9 kcal mol⁻¹, 9.9 kcal mol⁻¹ and -16.4 kcal mol⁻¹, respectively. The formation of the C-C bond from species **16** and **18** results in the intermediates **17** and **19** (Figs. S97 and S99 in the Supporting information) with relative enthalpies of 11.8 kcal mol⁻¹ and -12.1 kcal mol⁻¹, respectively. An alternative mechanism leads to the restoration of the double bond in the triazole (forming **20**), before the formation of the C-C bond. The presence of a strong base could restore the double bond of the alkene by hydrogen abstraction from the primary carbon of the alkene, promoting the elimination of the acetate ion. However, the energy profile for this alternative mechanism (Scheme 7) shows that it is not competitive with the route discussed below. Scheme 7 gives a summary of the relative enthalpies of the most relevant species we have discussed up to now. From here, we considered intermediates **13** and **14** as the key complexes to continue the reaction.

Intermediate **14** may be rearranged into **15**, as shown in Scheme 6e. From **15**, a reorientation in the structure, followed by a nucleophilic attack from the Pd-linked acetate oxygen to the primary carbon of the alkene, leads to the formation of intermediate **22** in a highly exothermic step (-34.7 kcal mol⁻¹). The activation barrier to form **22** was estimated by simulating the elongation of the Pd-C bond and calculating the energy for formation of a stable secondary carbocation, followed by a nucleophilic attack of the acetate oxygen on the carbocation (Scheme 6e). The relative enthalpy of **22**-*Carb* (8.0 kcal mol⁻¹) represents an upper limit to the activation enthalpy for this step.

The next step from intermediate **22** is the formation of the C-C bond between the naphthoquinone and the triazole (alkene), for which two routes were investigated. One route passes through intermediate **23**, again in a highly exothermic step (-39.6 kcal mol⁻¹), however with a high activation enthalpy (about 65 kcal mol⁻¹ relative to **22**) due the breaking of the bond between the acetate oxygen and the primary carbon of the alkene group forming a primary carbocation (**23-***Carb***).

The second reaction route involves restoring the double bond by deprotonation of the acetate to form the stable intermediate **24** (Scheme 7), an exothermic process by 5.4 kcal mol⁻¹. The formation of the C-C bond leading to intermediate **25** is endothermic by 37.8 kcal mol⁻¹ (-1.3 kcal mol⁻¹ relative to reactants) with activation enthalpy of 38.1 kcal

mol^{-1} (-1.0 kcal mol^{-1} relative to reactants). Pi stacking interactions between the arene and the naphthoquinone are the driving forces leading to the formation of the new C-C bond.

To complete the catalytic cycle, we calculated structures leading to restoration of the catalyst. This may happen by breaking the acetate-triazole bond, generating the intermediate **26** (-35.3 kcal mol^{-1}), followed by the rupture of the coordination between the coupling product and the catalyst metal (**24 + 7a**, -45.2 kcal mol^{-1}). Finally, the hydrobromic acid is eliminated for the complete restoration of the palladium acetate. It is interesting to know that the optimized structures **26** and **27** already had the hydrogen in the acetate facing to the bromine ion, culminating in the elimination of this acid for full restoration of the catalyst.
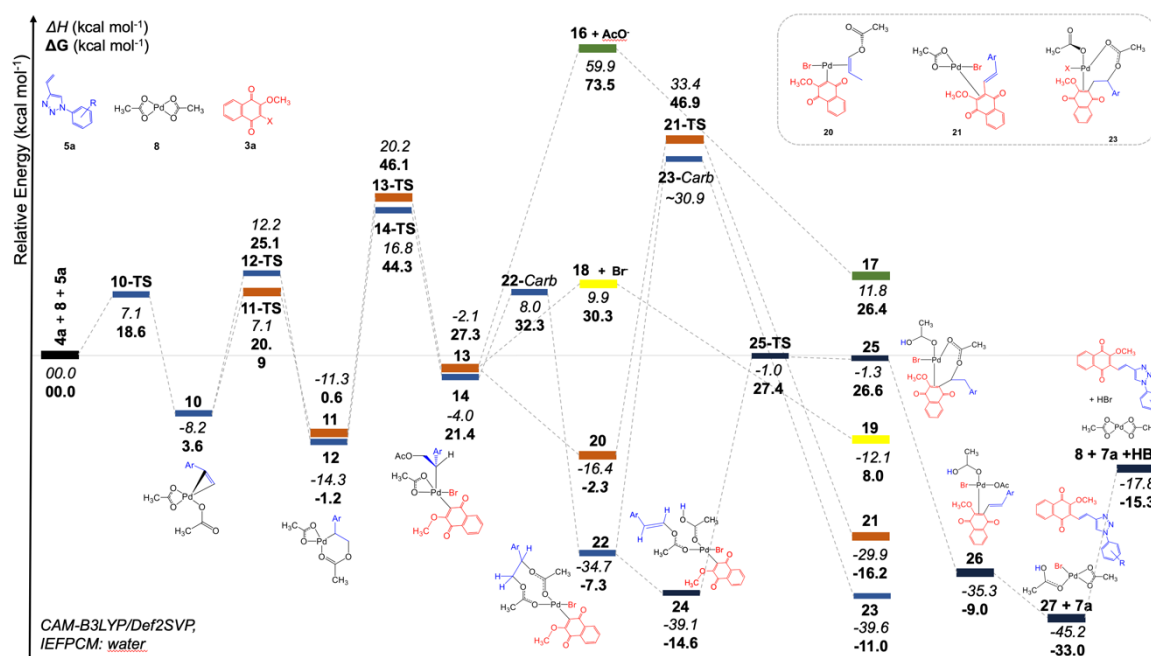
Scheme 7. Energy profile of the general mechanism involving the formation of the palladacycle intermediate proposed by Yao *et al*.[42]

The energy profile for the investigated mechanisms shows two important steps: the oxidative addition of the naphthoquinone (**12→14-TS**, Scheme 7) and the C-C bond forming steps (**24→25-TS**, Scheme 7). To identify the TOF-determining step (or steps) for this catalytic process and obtain insight into the experimentally observed selectivity for distinct reactants, theoretical TOF (turnover frequency) was estimated by calculating the energy span (δE) for the overall process, as proposed by Kozuchi and Shaik. [42] According to this approach the highest and the lowest energy points in the most favorable mechanism

– the TOF-determining energy transition state (TDTS) and the TOF-determining intermediate (TDI), respectively – are identified and used to calculate the overall energy barrier for the catalytic cycle. Here, we chose to compare the energy span values for distinct reactants and their respective catalytic cycles. Initially, the main points on the energy map shown in Scheme 7 were considered. Next, the influence of electron-withdrawing (**5d**) and electron-donating substituents (**5b** and **5c**) in the 4-vinyl-1*H*-1,2,3-triazoles derivatives were considered. The stationary points considered are the transition structures of highest enthalpy in the proposed mechanism (**14-TS** and **25-TS**) and the most stable intermediates (**12** and **24**). Each intermediate and transition states were reoptimized using the substituents mentioned above and the results are given in Table 3.

We computed the energy span (δE) using enthalpy of a common TOF-determining intermediate (**24**) and TOF-determining transition state (**25-TS**) for all substituents. The same TOF-determining intermediate (**24**) and TOF-determining transition state (**25-TS**) for **5a**, **5b** and **5c** were employed to compute the energy span (δE) based on the Gibbs free energy. For derivative **5d**, the δE depends on the TOF-determining intermediate **12** and the TOF-determining transition state **14-TS**. All the energy span (δE) values are summarized in Table 3. The relative stabilities and activation enthalpies of the main intermediates for the substituted derivatives do not significantly change as compared to the unsubstituted system. This is in contrast with the remarkably different experimental data for the different substituents. Other factors (*e.g.* distinct physical-chemical properties and losses during workup) rather than changes in the energy barriers may be the reason for the experimental observations. Nevertheless, the high energy spans obtained here are consistent with the high temperatures used in the synthesis (90-100ºC).

Table 3. Relative enthalpy and Gibbs free-energy (kcal mol^{-1}) of **12** and **24**, transition structures **14-TS** and **25-TS** as obtained for mechanism A. Energy span values (**δE**, kcal mol^{-1}) calculated according to Kozuchi and Shaik.[42]

R		12	14-TS	24	25-TS	δE (12 → 14-TS)	δE (24 → 25-TS)
H	ΔH	-14.3	16.8	-39.1	-1.0	31.1	38.1[a]
	ΔG	**-1.2**	**44.3**	**-14.6**	**27.4**	**45.5**[b]	**42.0**
CH₃	ΔH	-14.3	13.3	-39.2	-1.1	27.6	38.1[a]
	ΔG	**-1.3**	**40.9**	**-14.9**	**27.3**	**42.3**[b]	**42.2**
OCH₃	ΔH	-14.3	16.8	-39.9	-1.3	31.1	38.6[a]
	ΔG	**-0.9**	**44.7**	**-14.0**	**27.5**	**45.6**[b]	**41.5**

		12	14-TS	24	25-TS	δE (12 → 14-TS)	δE (24 → 25-TS)
NO₂	ΔH	-14.5	13.4	-38.4	-0.5	27.9	37.9 [a]
	ΔG	**-0.9**	**40.6**	**-14.1**	**28.0**	**41.4**	**42.1** [b]

[a]Identified rate-determining step when considering enthalpy change;

[b]Identified rate-determining step when considering Gibbs free- energy change.

Additionally, we investigated the effect of the halide bonded to the naphthoquinone on the calculated energy span. The transitions structures with the highest enthalpy (**14-TS** and **25-TS**) and the most stable intermediates (**12** and **24**, Table 3) were reoptimized replacing **-Br** by **-I**, for the parent system. The relative enthalpy and Gibbs free energy values obtained with **-I** instead of **-Br** are shown in Table 4. For 2-methoxy-3-bromo-1,4-naphthoquinone (**3a**), the TOF-determining step is **24 → 25-TS** (for δE determined by the enthalpy change), or **12 → 14-TS** (for δE determined by the Gibbs free-energy change). For 2-methoxy-3-iodo-1,4-naphthoquinone (**3b**), the TOF-determining step is **24 → 25-TS** (for δE determined by either the enthalpy change or the Gibbs free-energy change). It is important to highlight that the energy barrier for breaking the carbon-halogen bond (**14-TS**) has a considerable decrease when going from **-Br** to **-I**. Consequently, **12 → 14-TS** does not participate in the TOF-determining step for **3b**. This agrees with the observation that the reaction goes faster with iodine than with bromine bonded to the naphthoquinone ring. The energy span value is the same for **3a** and **3b**, when it is computed using the Gibbs free energy. When it is computed using the enthalpy, the δE for **3b** is about 3 kcal mol⁻¹ higher than for **3a**

Table 4. Relative enthalpy and Gibbs free-energy (kcal mol⁻¹) of **12** and **24**, transition structures **14-TS** and **25-TS** as obtained for mechanism A considering both 2-methoxy-3-bromo-1,4-naphthoquinone (**3a**) and 2-methoxy-3-iodo-1,4-naphthoquinone (**3b**). Energy span values (**δE**, kcal mol⁻¹) calculated according to Kozuchi and Shaik.[42]

		12	14-TS	24	25-TS	δE (12 → 14-TS)	δE (24 → 25-TS)
5a	ΔH	-14.3	16.8	-39.1	-1.0	31.1	38.1[a]
(C₃-Br)	**ΔG**	**-1.2**	**44.3**	**-14.6**	**27.4**	**45.5**[b]	**42.0**
5b	ΔH	-14.3	7.5	-41.2	0.0	21.7	41.2[a]
(C₃-I)	**ΔG**	**-1.2**	**35.0**	**-17.0**	**28.5**	**36.2**	**45.5**[b]

[a]Identified rate-determining step when considering enthalpy variation;

[b]Identified rate-determining step when considering Gibbs free- energy variation.

Conclusions

In conclusion, in this work, we achieved the first stereoselective, base- and ligand-free Heck coupling between naphthoquinones and 1*H*-1,2,3-triazoles to synthetize new conjugated naphthoquinone-triazole derivatives. All the Heck reactions with PEG-400 were stereoselective, generating only the (*E*)-isomers in good to excellent yields. This method provides a new platform for synthesizing other C-C conjugates of two important bioactive moieties, enabling further studies of possible molecular synergism. Computation shows that a mechanism where the first step is the coordination of the palladium acetate to the alkene is exothermic and occurs with low activation enthalpy being favored when compared to the classical insertion into the C-X bond of the naphthoquinone. After forming a palladacycle intermediate, the reaction evolves to the coupling with the naphthoquinone and formation of the C-C bond in the rate determining step, with *ca.* 38 kcal mol^{-1} activation enthalpy. The catalyst is thus regenerated by breaking the acetate-triazole bond, followed by the rupture of the coordination between the coupling product and the catalyst metal. Analysis of the substituent effects using the Kozuchi-Shaik model does not reveal any significative difference for the tested substituents.

Acknowledgements

References

[1] F. C. Silva, V. F. Ferreira *Curr. Org. Synth.* **2016**, *13*, 334-371.

[2] B. C. Zorzanelli, L. N. Queiroz, R. M. A. Santos, L. M. Menezes, F. C. Gomes, V. F. Ferreira, F. C. da Silva, B. K. Robbs *Fut. Med. Chem.* **2018**, *10*, 1141-1157.

[3] C. A. Camara, T. M. Silva, T. G. da-Silva, R. M. Martins, T. P. Barbosa, A. C. Pinto, M. D. Vargas *An. Acad. Bras. Ciênc.* **2008**, *80*, 329-334.

[4] T. P. Barbosa, C. A. Camara, T. M. S. Silva, R. M. Martins, A. C. Pinto, M. D. Vargas *Bioorg. Med. Chem.* **2005**, *13*, 6464-6469.

[5] V. F. Ferreira, A. Jorqueira, A. M. T. Souza, M. N. da Silva, M. C. B. V. de Souza, R. M. Gouvea, C. R. Rodrigues, A. V. Pinto, H. C. Castro, D. O. Santos, H. P. Araújo, S. C. Bourguignon *Bioorg. Med. Chem.* **2006**, *14*, 5459-5466.

[6] A. Jorqueira, R. M. Gouvea, V. F. Ferreira, M. N. da Silva, M. C. B. V. de Souza, A. A. Zuma, D. F. B. Cavalcanti, H. P. Araújo, S. C. Bourguignon *Parasitol. Res*. **2006**, *99*, 429-433.

[7] E. N. Silva Jr., R. F. S. Menna-Barreto, M. C. F. R. Pinto, R. S. F. Silva, D. V. Teixeira, M. C. B. V. de Souza, C. A. Simone, S. L. de Castro, V. F. Ferreira, A. V. Pinto *Eur. J. Med. Chem.* **2008**, *43*, 1774-1780.

[8] P. F. Carneiro, M. C. Pinto, R. K. F. Marra, F. C. da Silva, J. A. Resende, L. F. R. Silva, H. G. Alves, G. S. Barbosa, M. C. de Vasconcellos, E. S. Lima, A. M. Pohlit, V. F. Ferreira *Eur. J. Med. Chem.* **2016**, *108*, 134-140.

[9] L. M. Monteiro, R. Löbenberg, P. C. Cotrim, G. L. B. de Araujo, N. Bou-Chacra, *BioMed Res. Int.* **2017**, ID9781603.

[10] Y. X. Guo, L. Liu, D. Z. Yan, J. P. Guo *Mol. Med. Rep.* **2017**, *15*, 2333-2338.

[11] R. S. Brilhante, E. P. Caetano, R. A. Lima, F. J. Marques, D. S. Castelo-Branco, C. V. Melo, G. M. Guedes, J. S. Oliveira, Z. P. Camargo, J. L. Moreira, A. J. Monteiro, T. J. Bandeira, R. A. Cordeiro, M. F. Rocha, J. J. Sidrim *Braz. J. Microbiol.* **2016**, *47*, 917-924.

[12] M. de Barros, P. G. Perciano, M. H. dos Santos, L. L. de Oliveira, E. D. Costa, M. A. S. Moreira *Molecules* **2017**, *22*, E823.

[13] M. F. Cardoso, K. Salomão, A. C. Bombaça, D. R. da Rocha, F. C. da Silva, J. A. S. Cavaleiro, S. L. de Castro, V. F. Ferreira *Bioorg. Med. Chem.* **2015**, *23*, 4763-4768.

[14] D. Dheer, V. Singh, R. Shankar *Bioorg. Chem.* **2017**, *71*, 30-54.

[15] L. S. M. Forezi, M. F. C. Cardoso, D. T. G. Gonzaga, F. C. Silva, V. F. Ferreira *Curr. Top. in Med. Chem.* **2018**, *18*, 1428-1453.

[16] S. G. Agalave, S. R. Maujan, V. S. Pore *Chem. Asian J.* **2011**, *6*, 2696-2718.

[17] D. Dheer, V. Singh, R. Shank *Bioorg. Chem.* **2017**, *71*, 30-54.

[18] A. K. Jordão, V. F. Ferreira, T. M. L. Souza, G. G. S. Faria, V. Machado, J. L. Abrantes, M. C. B. V. Souza, A. C. Cunha *Bioorg. Med. Chem.* **2011**, *19*, 1860-1865.

[19] I. F. Silva, P. R. C. Martins, E. G. Silva, S. B. Ferreira, V. F. Ferreira, K. R. C. Costa, M. C. Vasconcellos, E. S. Lima, F. C. da Silva *Med. Chem.* **2013**, *9,* 1085-1090.

[20] D. T. G. Gonzaga, L. B. G. Ferreira, T. E. M. M. Costa, N. L. von Ranke, P. A. F. Pacheco, A. P. S. Simões, J. C. Arruda, L. P. Dantas, H. R. Freitas, R. A. M. Reis, C. Penido, M. L. Bello, H. C. Castro, C. R. Rodrigues, V. F. Ferreira, R. X. Faria, F. C. Silva *Eur. J. Med. Chem.* **2017**, *139*, 698-717.

[21] S. M. M. Lopes, J. S. Novais, D. C. S. Costa, H. C. Castro, A. M. S. Figueiredo, V. F. Ferreira, T. M. V. D. M. Pinho, F. C. Silva *Eur. J. Med. Chem.* **2018**, *143*, 1010-1020.

[22] Y. Kommagalla, S. Cornea, R. Riehle, V. Torchilin, A. Degterev, C. V. Ramana *MedChemComm* **2014**, *5*, 1359-1363.

[23] G. Wei, W. Luan, S. Wang, S. Cui, F. Li, Y. Liu, Y. Liu and M. Cheng *Org. Biomol. Chem.* **2015**, *13*, 1507-1514.

[24] R. I. Filho, D. T. G. Gonzaga, T. M. Demaria, J. G. B. Leandro, D. C. S. Costa, V. F. Ferreira, M. Sola-Penna, F. C. da Silva, P. Zancan *Curr. Top. Med. Chem.* **2018**, *18*, 1483-1493.

[25] D. C. S. Costa, G. S. de Almeida, V. W.-H. Rabelo, L. M. Cabral, P. C. Sathler, P. Abreu, V. F. Ferreira, L. C. R. P. da Silva, F. C. da Silva *Eur. J. Med. Chem.* **2018**, *156*, 524-533.

[26] L. Scotti, F. J. B. Mendonca-Junior, M. T. Scotti *Curr. Top. Med. Chem.* **2017**, *17*, 843-844.

[27] F. C. Demidoff, F. P. Souza, C. D. Netto *Synthesis* **2017**, *49*, 5217-5223.

[28] F. C. Demidoff, E. J. P. R. Filho, A. L. F. Souza, C. D. Netto, L. L. Carvalho, *Synthesis* **2021**, *53*, 4097-4109.

[29] A. L. Perez, G. Lamoureux, B. Y. Zhen-Wu *Tetrahedron Lett.* **2007**, *48*, 3995-3998.

[30] L. F. Tietze, R. R. Singidi, K. M. Gericke *Chem. Eur. J.* **2007**, *13*, 9939-9947.

[31] A. L. Perez, G. Lamoureux, A. Herrera *Synth. Comm.* **2004**, *34*, 3389-3397.

[32] M. A. Gouda, H. F. Eldien, M. M. Girges, M. A. Berghot *Med. Chem.* **2013**, *3*, 228-232.

[33] J. Sharma, P. K. Singh, K. P. Singh, R. N. Khanna *Org Prep. Proc. Int.* **1995**, *27*, 84-86.

[34] N. Boechat, V. F. Ferreira, S. B. Ferreira, M. L. G. Ferreira, F. C. da Silva, M. M. Bastos, M. S. Costa, M. C. S. Lourenço, A. C. Pinto, A. U. Krettli, A. C. Aguiar, B. M. Teixeira, N. V. da Silva, P. R. C. Martins, F. A. F. M. Bezerra, A. L. S. Camilo, G. P. da Silva, C. C. P. Costa *J. Med. Chem.* **2011**, *54*, 5988-5999.

[35] R. Deshpande, L. Jiang, G. Schmidt, J. Rakovan, X. Wang, K. Wheeler, H. Wang, *Org. Lett.* **2009**, *11*, 4251-4253.

[36] L. S. M. Forezi, A. T. P. C. Gomes, M. G. P. M. S. Neves, V. F. Ferreira, F. C. S. Boechat, M. C. B. V. de Souza, J. A. S. Cavaleiro *Eur. J. Org. Chem.* **2015**, 5909-5913.

[37] W. Han, C. Liu, Z.-L. Jin *Org. Lett.* **2007**, *20*, 4005-4007.

[38] L. Yin, J. Liebscher *Chem. Rev.* **2007**, *107*, 133-173.

[39] A. Molnar *Chem. Rev.* **2011**, *111*, 2251-2320.

[40] Q. Yao, E. P. Kinney, Z. Yang *J. Org. Chem.* **2003**, *68*, 7528-7531.

[41] D. J. Jones, M. Lautens, G. P. McGlacken *Nat. Catal.* **2019**, *2*, 843-851.

[42] S. Kozuch, S. Shaik *J. Am. Chem. Soc.* **2006**, *128*, 3355-3365.